Optimization of PZT ceramic IDT sensors for health monitoring of structures

Rafatou Takpara, Marc Duquennoy, Mohammadi Ouaftouh, Christian Courtois, Frédéric Jenot, Mohamed Rguiti

Optimization of PZT ceramic IDT sensors for health monitoring ofstructures

Rafatou Takpara [a,b], Marc Duquennoy [a,*], Mohammadi Ouaftouh [a], Christian Courtois [b], Frédéric Jenot [a], Mohamed Rguiti [b]

[a] Univ. Valenciennes, CNRS, Univ. Lille, ISEN, Centrale Lille, UMR 8520 – IEMN, DOAE, F-59313 Valenciennes, France
[b] LMCPA, Université de Valenciennes et du Hainaut-Cambrésis, Pôle Universitaire de Maubeuge, France

Surface acoustic waves (SAW) are particularly suited to effectively monitoring and characterizing structural surfaces (condition of the surface, coating, thin layer, micro-cracks. . .) as their energy is localized on the surface, within approximately one wavelength. Conventionally, in non-destructive testing, wedge sensors are used to the generation guided waves but they are especially suited to flat surfaces and sized for a given type material (angle of refraction). Additionally, these sensors are quite expensive so it is quite difficult to leave the sensors permanently on the structure for its health monitoring. Therefore we are considering in this study, another type of ultrasonic sensors, able to generate SAW. These sensors are interdigital sensors or IDT sensors for InterDigital Transducer. This paper focuses on optimization of IDT sensors for non-destructive structural testing by using PZT ceramics. The challenge was to optimize the dimensional parameters of the IDT sensors in order to efficiently generate surface waves. Acoustic tests then confirmed these parameters.

1. Introduction

The operating principle of InterDigital Transducer (IDT) requires making electrodes several millimeters in length. However, the widths of these electrodes are extremely low, as they must correspond to a quarter of the wavelength. For example, with a PZT plate and a frequency of 10 MHz, the width of the electrodes must be 45 μm. It is possible to use microelectronics methods (Lift-off technology, for example) to make such electrodes with very high resolutions. However, depending on the nature of the piezoelectric materials and the number of sensors to be made, other methods based on laser ablation or inkjet printing can be envisaged. However, it is necessary to adapt them to the intrinsic characteristics of these materials and in particular their porosity and roughness [1]. Many papers have demonstrated the interest of IDT sensors for non-destructive testing [2–5], but few studies focus on optimizing the dimensional parameters of SAW-type surface wave ultrasonic sensors for structural health monitoring. The ability of several piezoelectric ceramics to generate SAW was tested using finite element modeling. Then, in order to generate high amplitude SAW, different designs were modeled to determine the most appropriate optimum dimensional characteristics. After making the sensors, acoustic tests confirmed the dimensional optimization of the IDT sensors.

* Corresponding author.
E-mail address: marc.duquennoy@univ-valenciennes.fr (M. Duquennoy).

2. Surface wave sensors

The development of IDT sensors is linked to the development of ultrasound techniques. The development of IDT sensor technology is marked by the discovery of the surface acoustic wave on one hand by Lord Rayleigh in 1885 [6] and by the beginning of large-scale research in 1965 on other hand, with the first achievement of the SAW device. This achievement comes from the need to improve the performance of existing radars by compressing its pulses. Today different SAW devices are used in professional applications in radar, televisions, mobile phones and all kinds of sensors (seismic, acousto-optical, etc.).

Main characteristic of SAW is that their energy is localized on the surface, within approximately one wavelength. Conventionally, triangular sections prisms are used to generate SAW [7]. SAW is generated by converting acoustic bulk waves (Snell- Descartes's Law) generated into the prism, itself placed on the surface on which SAW is excited. The prism is oriented at an angle θ_R, to have the horizontal component of the bulk wave velocity equals to the velocity of SAW of the underlying material. When this condition

is satisfied, there is a conversion of SAW into bulk wave. The prism angle being related to SAW velocity in the substrate, it is thus necessary to adapt the angle for each material.

Another method to generate SAW is to use a comb-shaped structure [7]. As for wedge sensors, piezoelectric element excites bulk waves which are converted into SAW through a periodic grating (alternation of salience and slot $\lambda_R/2$ in width). This type of sensor is capable of exciting very effectively Rayleigh wave by placing it at the surface of sample of any kind of materials. The condition for this kind of sensor is that the spatial periodicity of the comb should be equal to the wavelength λ_R [6]. In 1965, White et al. have suggested other IDT sensors with another way to deposit electrodes. Now interlinked electrodes are on piezoelectric plate directly. We have chosen to focus on this type of sensors. Indeed, we have possibility of developing sensors capable of generating surface waves over a broad frequency range [4], as well as conformable sensors [1] and finding solutions to significantly reduce manufacturing costs. Under these conditions, it is possible to envisage continuous control with the permanent integration of these sensors in the structures.

2.1. Operating principle of IDT sensors

An IDT sensor consists of two comb-shaped metal electrodes composed of interlinked fingers deposited on a piezoelectric plate (Fig. 1). When a voltage "U" is applied between the two electrodes, the field created generates compressions and dilatations near the surface of the piezoelectric plate, thus producing SAW. These waves are emitted each side of the sensor with a wave front parallel to the IDT sensor electrodes [8–10].

3. Modeling of SAW sensors

The IDT sensor parameters were optimized to achieve significant levels of displacement compatible with non-destructive testing. This optimization was performed using COMSOL Multiphysics® finite element analysis software. Since the displacement field generated by the SAW is contained in the sagittal plane XY (fig. 1) [9], it was possible to model the propagation of SAW in 2D, the medium being considered infinite in the third direction Z. This limited the number of nodes and thus significantly reduced the computation time. With the finite element method, the solution space is discretized into subdomains called elements. These elements are the elementary bricks and the mesh represents the geometrical system to be simulated. The elements are composed of several nodes. Linear quadrangular elements were used as they provide a uniform mesh. Concerning the size of these elements, various tests have shown that sizes smaller than or equal to "$\lambda_R/10$" are required to obtain good results (where λ_R is the wavelength of SAW). A time step equal to "T/20" was selected, where T is the period of the electrical excitation signal. The full computation time T_c was calculated by adding the time of the electrical excitation signal to the time of propagation of the SAW waves in the plate. The propagation of the waves can thus be observed in the structure. For all the models, attenuation was not considered. This simplification only affects (not very meaningfully) the displacement amplitude. Indeed, the dimensions of the surfaces modeled were small in order to limit the number of nodes and thus the computation time.

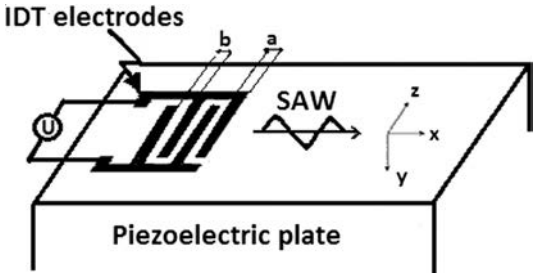

Fig. 1. Diagram of an IDT sensor.

4. Ability of different piezoelectric ceramic for SAW generation

In the first time, different PZT piezoelectric ceramics were tested to determine their ability to generate SAW (Pz26, Pz27, Pz29 [11], BM500, BM532 [12], P191 [13]).

The model used in this section consists of three blocks: the piezoelectric plate on which the SAW is generated, and two dampers located on either side. In this model, "a" denotes the width of the electrodes, "b" the spacing between the electrodes (Fig. 1), "e" the thickness of the piezoelectric plate and "P1" the point where the displacements are recorded (Fig. 4). The thickness "e" of the plate was chosen to be sufficiently large in relation to the wavelength ($e \approx 10 \cdot \lambda_R$) to be in the right conditions for Rayleigh wave propagation. Finally, there are five pairs of electrodes on the piezoelectric plate (Fig. 2). In this paper, bidirectional IDT sensors are considered and the electrodes are spaced half a wavelength apart, which corresponds to the central operating frequency ($a + b = \lambda_R/2$). The width of the electrodes is equal to a quarter of a wavelength ($a = b = \lambda_R/4$).

The dampers' role is to prevent the inadvertent return of reflected waves at the ends of the plate. These dampers have the same mechanical properties as the piezoelectric plate to avoid any reflection related to the rupture of the acoustic impedance at the interfaces between the piezoelectric plate and these dampers, but the latter must provide significant attenuation.

Different electrical excitations can be applied to these interdigital electrodes (pulse, burst, chirp), but in this paper "burst" type excitations were presented, as they are commonly used in experiments. Indeed, by applying a sufficient number of sinusoids with amplitudes of several tens of volts, the amplitude of the surface waves generated enable measurements to be conducted on most materials without the attenuation being too high.

Knowing that the maximum displacement amplitude generated by the surface waves is obtained for a number of sinusoids higher than or equal to the number of electrode pairs [4], a "burst" electrical excitation consisting of ten sinusoids with a peak amplitude of 20 V and a frequency of 20 MHz was systematically applied to the five pairs of IDT sensor electrodes. This configuration makes it possible to analyze the sensor performance in terms of displacement amplitude of the surface waves generated while limiting the duration of echoes and thus the computation time.

4.1. Estimation of displacements

Fig. 2 presents an example of modeling results where it is possible to observe the surface wave generation.

It should be noted that the electrodes are represented by lines on the upper surface of the piezoelectric plate. The influence of their mass is negligible in relation to the thickness of the plate. The displacement fields (in the x direction) are represented by color levels. In this example, the maximum amplitude of the SAW is 32 nm. The effectiveness of the dampers can be observed since SAW are firstly absorbed then completely attenuated.

Normal displacements (at point P1) generated by the surface wave propagating on a Pz29 piezoelectric plate are shown in fig. 3. As expected, a plateau (32 nm) can be observed from the 5th sinusoidal as there are five pairs of electrodes.

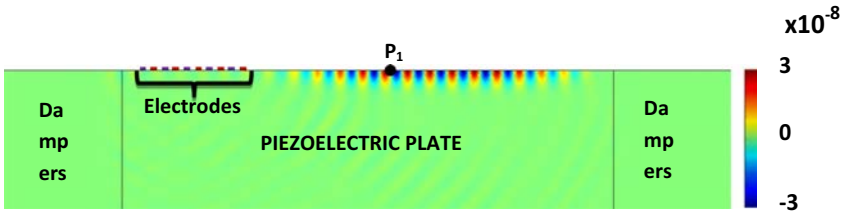

Fig. 2. Generation of SAW on IDT sensor (t = 16 × T = 800 ns).

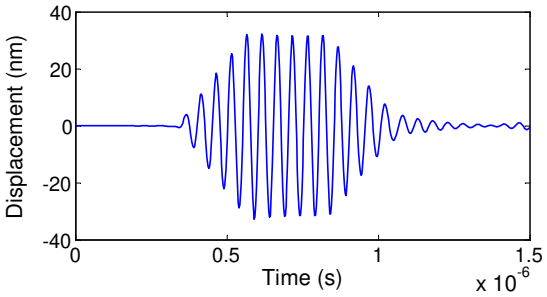

Fig. 3. Normal displacements (in Y direction) generated at P1 on IDT sensor.

For the judicious comparison of the amplitudes for each PZT plate, we took small fluctuations in amplitude pulses into account. This allows the displacements of the piezoelectric plates to be estimated with a precision of ±0.7 nm. This method will also be used to estimate the maximum displacement amplitudes in the study of the generation of surface waves on a non-piezoelectric substrate using an IDT sensor.

Table 1 summarizes the parameters used to calculate the maximum amplitudes of normal displacements (Y direction) obtained for IDT piezoelectric sensors made up of different PZT piezoelectric plates. The results are ranked from the most efficient (the one that generates the highest displacement) to the least efficient (the one that generates the lowest displacement).

This result highlights ceramics are of interest for this type of sensors, as amplitudes are sizable for surfaces wave. It should be noted that the frequencies used conventionally in SAW sensors applications (electronic filters) are hundreds megahertz or a few gigahertz. In that case, it is better to consider single crystals rather than PZT materials. In NDT applications referred here, the frequency range is between 1 and 100 MHz.

5. Modeling of IDT sensors put on the substrate

The previous model was used to study the generation of surface waves by an IDT sensor, the surface waves propagating directly on the surface of the piezoelectric plate constituting the sensor. This study is not sufficient because, contrary to a surface-wave filter, it is necessary to propagate SAW on the structure in order to control its cortical features or its coating. In addition, we also plan to leave the sensors permanently on the structure to be characterized. It is therefore necessary to supplement this study taking into account the influence of the structure, which will be named "substrate" hereinafter.

The model used in this section consists of a piezoelectric plate put on the substrate on which the SAW needs to be propagated. As before, two dampers were positioned at both ends of the substrate to prevent the unwanted return of waves propagating at the left end of the piezoelectric plate, and the two ends of the substrate (Fig. 4). These precautions are necessary in the model, as the surfaces modeled are very small (number of nodes). However, the plate and the substrate are big enough in the experimental phase and there are no harmful wave reflections.

The simulation model used to generate surface waves on the substrate is shown in fig. 4. e is the thickness of the piezoelectric plate, e' the thickness of the substrate and P2 the point on the substrate where the displacements are recorded.

Experimentally, the sensor can be either glued (permanently) to the structure or placed on substrate via a couplant. These two configurations can be modeled by simulation either zero degrees of freedom (continuity of constraint and displacement at the interface) or free sliding in XZ plane between both of the materials, but no couplant is considered in simulation.

Fig. 5 shows results of the simulation for these two kinds of links, for Pz29/aluminum. Displacements recorded in both two cases are comparable in shape and amplitude since maximum amplitudes of displacements are 15 nm and 14 nm for the bonded case and non-bonded case respectively. Considering this small difference, for further simulations, only the rigid link (sensor bonded to the substrate) will be considered for the next simulations.

The quality of the generation of surface waves on the substrate from an IDT sensor is governed by several parameters such as the geometry of the piezoelectric plate (length and thickness), the geometry of the electrodes and finally by intrinsic proprieties of both the plate (electric proprieties, elastic and piezoelectric constants) and the substrate (elastic proprieties). At first, the thickness of the piezoelectric plate is considered.

5.1. Study of the ideal thickness for the piezoelectric plate of an IDT sensor

Given the results obtained previously on the piezoelectric plates, the characteristics of the PZT selected for modeling correspond to those of Pz29. Aluminum was chosen as the substrate,

Table 1
Maximum amplitudes of normal displacements (Y direction) generated on IDT sensor.

Classification	Material	Displacement at P_1 (nm)	Width of electrodes (μm)	Frequency (MHz)
1	Pz29	32	22	20
2	BM500	28.5	22	20
3	BM532	28.4	22	20
4	Pz27	21.1	22	20
5	P191	15.9	25	20
6	Pz26	13	25	20

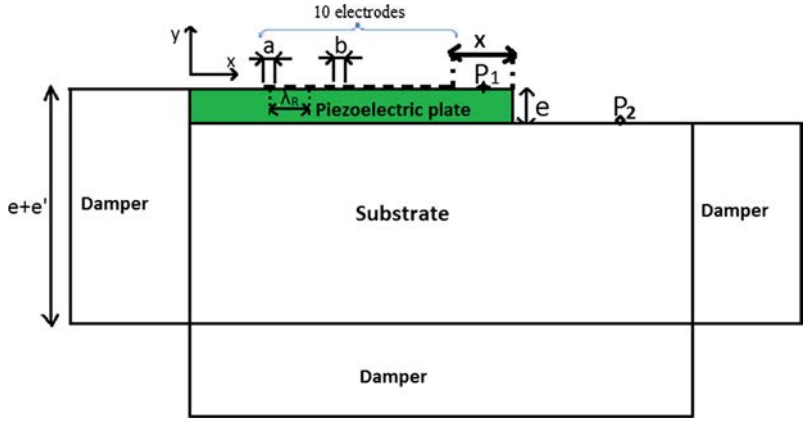

Fig. 4. Model used to study SAW, generated by IDT sensor, on substrate.

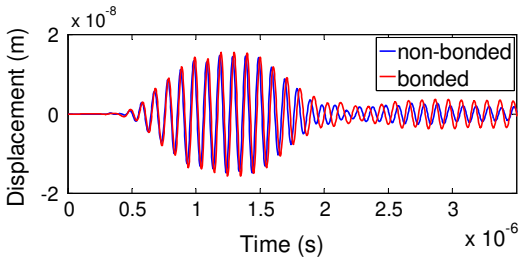

Fig. 5. Normal displacements generated at P2 for bonded and *non-bonded* IDT sensors on aluminum substrate.

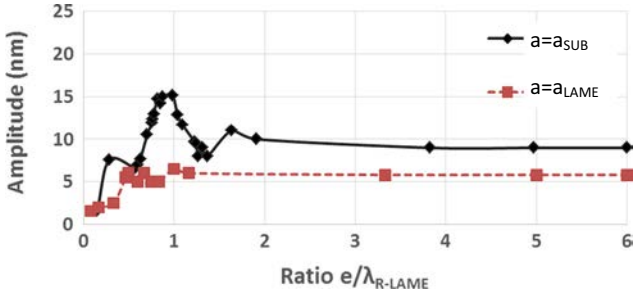

Fig. 6. Maximum displacement amplitudes generated at P_2 with an IDT sensor, depending on the thickness of the piezoelectric plate.

as it often has to be controlled, particularly when used in the aerospace industry.

A classical IDT sensor of which the width of the electrodes a is equal to the spacing between the electrodes b, meets the following condition with regard to the wavelength λ_R (Fig. 1):

$$\lambda_R = \frac{V_R}{f} = 2 * (a + b), \quad \text{with a} = \text{b} \tag{1}$$

where V_R is SAW velocity.

This condition enables the periodicity of the electrodes to be adapted to the wavelength of the piezoelectric material for a given sensor Eigen frequency, and allows a high amplitude surface wave to be obtained. This problem is now impeded by the fact that the SAW must be generated on the substrate of which the elastic characteristics are different from those of the plate. In other words, two SAW propagation velocities must be taken into account: the first one in the substrate (V_{R_SUB}) and the second one in the piezoelectric plate (V_{R_LAME}). Therefore, we need to know if it is better to adapt the periodicity of the electrodes to the wavelength of the surface wave in the piezoelectric plate ($\lambda_{R\text{-}LAME}$) or in the substrate ($\lambda_{R\text{-}SUB}$).

There are two possibilities for making the electrodes: the width a of the electrodes is adapted to either V_{R_SUB} or V_{R_LAME}:

$$\text{1st case}: \quad a_{SUB} = \lambda_{R\text{-}SUB}/4 = \frac{V_{R\text{-}SUB}}{4.f}; \tag{2}$$

$$\text{2nd case}: \quad a_{LAME} = \lambda_{R\text{-}LAME/4} = \frac{V_{R\text{-}LAME}}{4.f}; \tag{3}$$

These two cases were investigated in simulation with different piezoelectric plate thicknesses. This is extremely important as it determines the distribution of the acoustic energy in the plate.

The maximum displacement amplitudes generated on the substrate are reported in fig. 6. Electrical excitation is still a "burst" (ten sinusoids, 20 V peak, 10 MHz). The black curve (dashes) was obtained for a_{SUB} and the red curve for a_{LAME}. In both cases, the results are reported with the ratio between the piezoelectric plate thickness and the Rayleigh wave wavelength in the piezoelectric plate on the abscissa.

The results clearly show that when the width of the electrode is adapted to the wavelength of the surface wave of the substrate ($a = \lambda_{R\text{-}SUB}/4$), the amplitude of the displacements generated by the surface wave in the substrate is much higher than in the case where $a = \lambda_{R\text{-}LAME}/4$, regardless of the plate thickness. The optimal piezoelectric plate thickness corresponds to the wavelength of the surface wave in the plate. For a −3 dB attenuation around this maximum value, it is considered better to choose a $e/\lambda_{R\text{-}LAME}$ ratio between 0.8 and 1.2, and therefore choose a thickness comparable to the Raleigh wave wavelength in the plate.

Under these conditions, three areas were studied corresponding to $0.8 < e/\lambda < 1.2$; $e/\lambda < 0.8$ and $e/\lambda > 1.2$, and are described in the following paragraphs.

5.1.1. Ratio corresponding to $0.8 \leq e/\lambda_{R\text{-}LAME} \leq 1.2$

In this first case, the thickness is comparable to the wavelength of the SAW in the piezoelectric plate. Thus, when a voltage is applied between the electrodes, a displacement field is immediately created throughout the thickness of the plate. The displacements are transmitted to the substrate and with each electrical impulse it is possible to observe the wave forming at the interface (Fig. 7(a)), then, the SAW progresses beyond the piezoelectric plate, on the substrate (Fig. 7(b)). Displacements related to the generation of bulk waves correspond to losses, and it is possible to observe that these two contributions (surface and bulk waves) rapidly split up. Under these conditions, the SAW propagate on the substrate without being disrupted by other contributions (bulk waves).

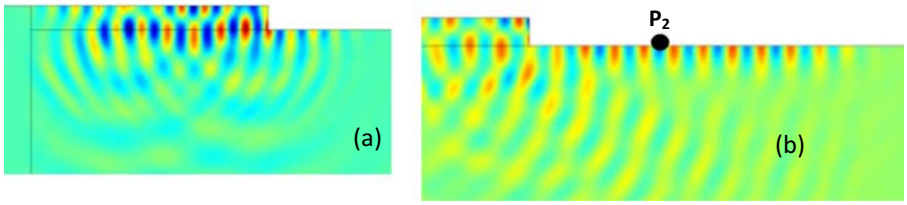

Fig. 7. Displacements (in Y direction) for e = $\lambda_{R\text{-}LAME}$ (a) t = 5 · T and (b) t = 15 · T.

As shown on the curve in fig. 6, in this interval, displacement amplitudes are high for thicknesses corresponding to e ≈ $\lambda_{R\text{-}LAME}$, and then decrease either side of this value. Effective SAW generation is also confirmed by the shape of the displacement signal that is the same at any point on the substrate. In addition, it is possible to deduce the SAW velocity by measuring the signal at different positions on the substrate. The SAW velocity calculated was 2863 m/s. This value corresponds to the SAW velocity in aluminum.

5.1.2. Ratio corresponding to e/$\lambda_{R\text{-}LAME}$ ≤ 0.8

In this second case, the thickness of the plate is lower than the SAW wavelength $\lambda_{R\text{-}LAME}$. Thus, when a voltage is applied to the electrodes, the displacement field is immediately transmitted to the substrate and the distribution is directly related to the position and the polarity of the electrodes. Then, this contribution continues with the electrical impulses (Fig. 8(a)). A significant part of the energy contributes to the generation of bulk waves and a smaller portion of this energy is localized on the surface. However, contrary to the previous case (0.8 ≤ e/$\lambda_{R\text{-}LAME}$ ≤ 1.2), where the generation of a SAW can clearly be seen, the displacement field is not typical of SAW and in particular the attenuation of the displacement in relation to the depth (Fig. 8(b)). The shape of the displacement signal on the surface of the substrate is also different at different points. Finally, it should be noted that this phenomenon varies considerably according to the thickness.

Fig. 9 shows an example of the displacement signal observed at P_2 for these small thickness (e = 28 μm). This does not correspond to the displacement obtained when SAW were generated on a piezoelectric plate (Fig. 3), and the shape of this signal varies from one point to another. There is clearly more wave mixing. In addition, according to the thickness, these interferences are more or less favorable. However, overall it is better to consider the previous case.

5.1.3. Ratio corresponding to e/$\lambda_{R\text{-}LAME}$ ≥ 1.2

In this third case, the thickness of the plate is greater than the wavelength of the surface wave. Two cases can be distinguished because two different behaviors can be observed depending on a (a = $\lambda_{R\text{-}SUB}$/4 and a = $\lambda_{R\text{-}LAME}$/4).

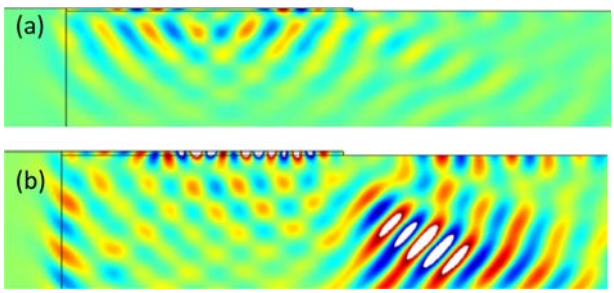

Fig. 8. Displacements (in Y displacement) for e/$\lambda_{R\text{-}LAME}$ = 0.15 (a) t = 5 · T and (b) t = 15 · T.

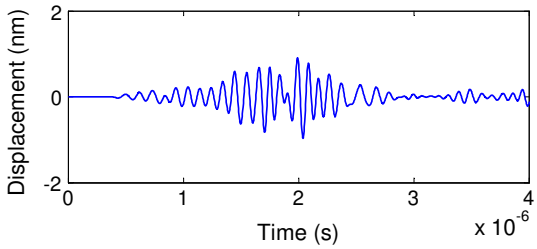

Fig. 9. Normal displacements (in Y direction) generated at P2 for e/$\lambda_{R\text{-}LAME}$ = 0.15.

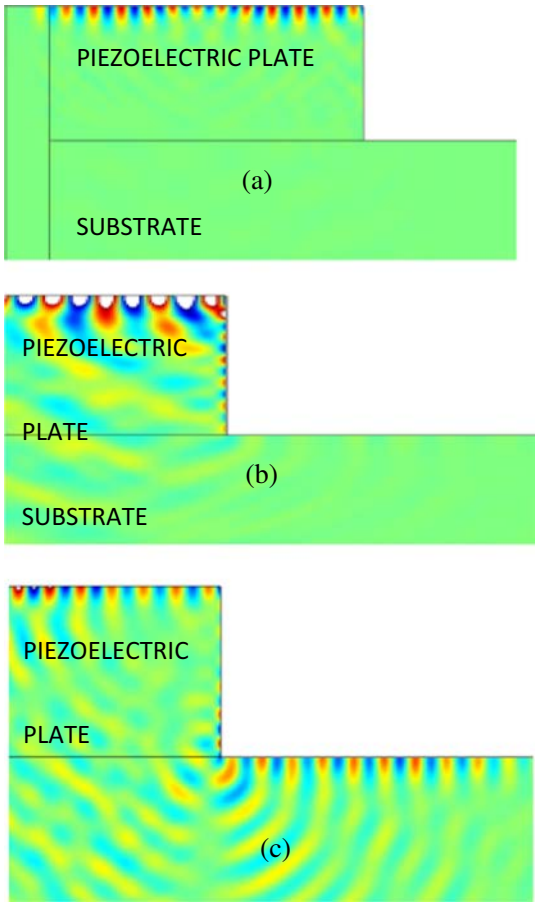

Fig. 10. Displacements (in Y displacement) for e/$\lambda_{R\text{-}LAME}$ = 5, with a = $\lambda_{R\text{-}LAME}$/4 (a) t = 10 · T, (b) t = 15 · T and (c) t = 20 · T.

5.1.3.1. 1st case: a = $\lambda_{R\text{-}LAME}$/4. The thickness being sufficiently large, when *a* = $\lambda_{R\text{-}LAME}$/4, SAW are first generated on the plate (Fig. 10 (a)), then bypass the edge of the plate (Fig. 10(b)), and finally propagate on the substrate (Fig. 10(a)).

To highlight the strong influence of the piezoelectric plate edge, another model was used which differs from the previous one by

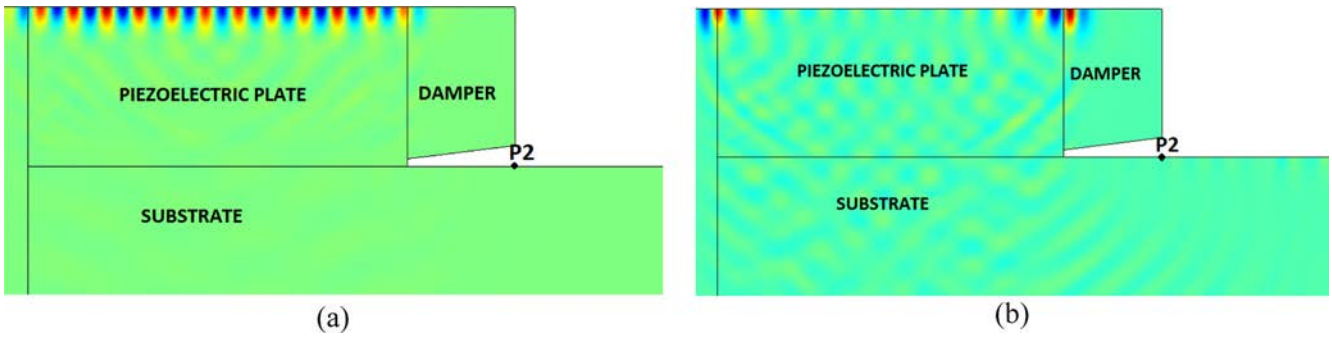

Fig. 11. Displacements (in Y displacement) for $e = 5 \cdot \lambda_{R\_LAME}$; (a) $t = 5 \cdot T$ and (b) $t = 15 \cdot T$.

the addition of a damper at the edge of the piezoelectric plate. This damper was optimized because it must be very close to the substrate to absorb any contributions that pass through the edge of the piezoelectric plate, but without being in contact with the substrate to avoid absorbing the surface wave propagating on the latter (Fig. 11).

The displacements recorded with and without damper and for the same thickness ($e = 5 \cdot \lambda_{R\_LAME}$) confirm that all the energy goes through the edge of the piezoelectric plate (Fig. 12). An IDT sensor with such parameters (i.e., $e/\lambda_{R\text{-}LAME} \geq 1.2$ and $a = \lambda_{R\_LAME}/4$) is numerically effective because the edge can be schematized perfectly. However, in reality it would be difficult to obtain a piezoelectric plate with perfect edges. As the amplitudes are lower, it is better to use the 1st case if possible.

5.1.3.2. 2nd case: $a = \lambda_{R\text{-}SUB}/4$. When $a = \lambda_{R\text{-}SUB}/4$, the periodicity of the electrodes no longer meets the conditions for generating surface waves on the plate. However, the results (Fig. 6) show that this case is preferable for large thicknesses. The modeling shows that most of the displacements are related to bulk waves that initially propagate in the piezoelectric plate. A very small part of the energy participates in the generation of a surface wave. These waves propagate in the volume of the piezoelectric plate at an angle θ_c, as shown in fig. 13, and are transmitted to the substrate. Depending on the length and the thickness of the plate, these waves may or may not reach the edge of the plate.

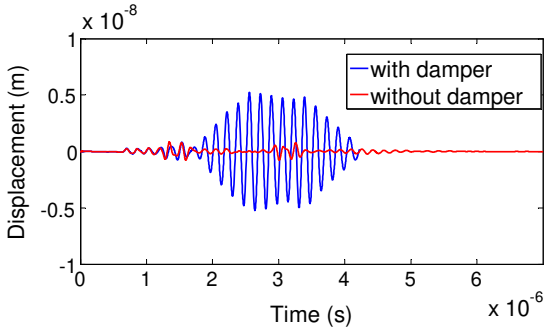

Fig. 12. Normal displacements (in Y direction) generated at P_2 without damper and with damper, for $a = \lambda_{R\_LAME}/4$ and $e = 5 \cdot \lambda_{R\_LAME}$.

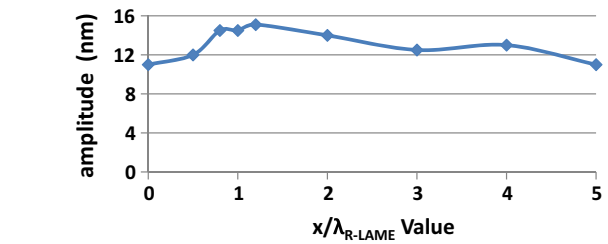

Fig. 14. Maximum displacement amplitudes generated at P2 for $e = \lambda_{R\text{-}LAME}$ depending on X distance.

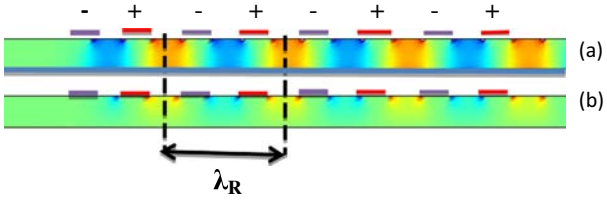

Fig. 15. Y-axis component of the field lines for $e/\lambda_{R\text{-}LAME} = 0.28$ (a) with ground electrode (b) without ground electrode.

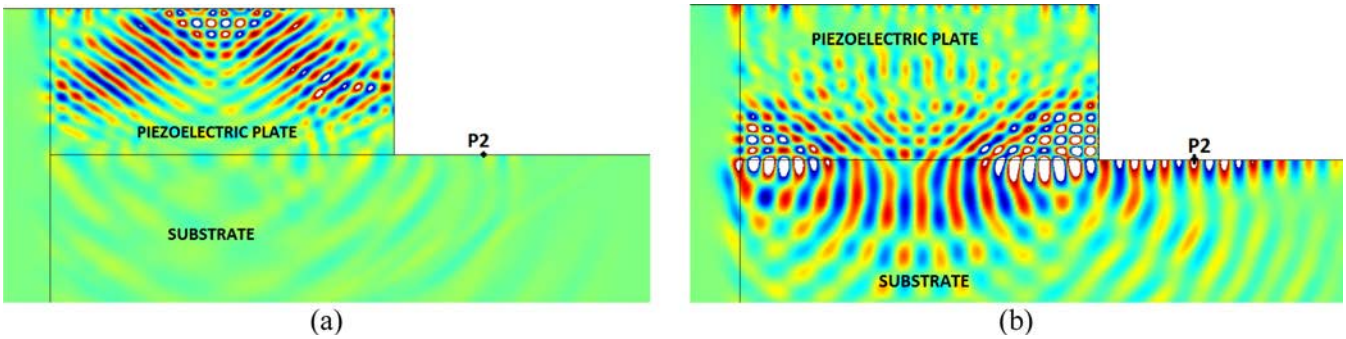

Fig. 13. Displacements (in Y displacement) for $e = 5 \cdot \lambda_{R\_LAME}$ and $a = \lambda_{R\_LAME}/4$ (a) $t = 10 \cdot T$ and (b) $t = 20 \cdot T$.

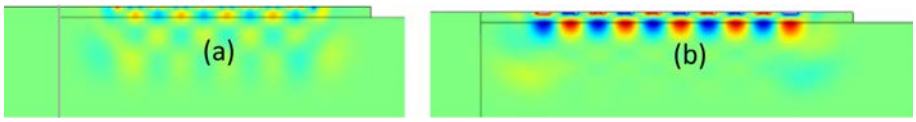

Fig. 16. Displacements (in Y displacement) for $e/\lambda_{R\text{-}LAME} = 0.28$ (a) without ground electrode (b) with ground electrode.

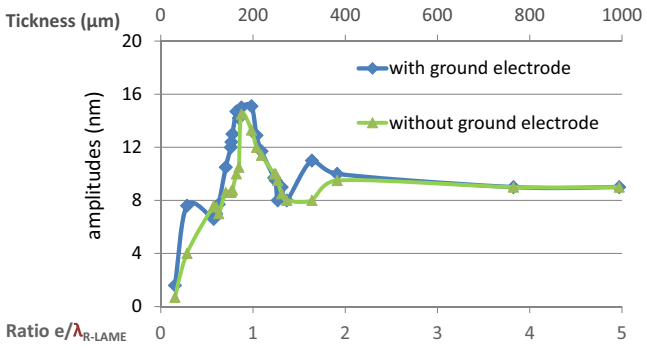

Fig. 17. Maximum displacement amplitudes of SAW generated at P_2 with and without ground electrode according to the ration e/λ_{R_LAME}.

5.2. Influence of the length of the piezoelectric plate

Given the above observations, it is better to consider a thickness of plate comparable to λ_{R_LAME} but in that case, it was necessary to check the influence of the position of the edge of the piezoelectric plate. Assuming that X is the distance between the electrodes and the edge of the piezoelectric plate (Fig. 4), different lengths of piezoelectric plate were considered for a thickness equal to the wavelength. The maximum displacement amplitude was attained for $X \approx 1.2 \cdot \lambda_{R\text{-}LAME}$ (Fig. 14). However, the value of X does influence a lot the shape or amplitude of the displacements generated.

5.3. Influence of a ground electrode

Conventionally, IDT sensor electrodes are only placed on the upper surface of the piezoelectric plate. In this case, the electrical voltage applied between the two electrodes creates an electric field and therefore displacement within a limited area beneath the surface. However, some authors have proposed an additional electrode on the bottom surface [2,3,5]. We verified if this additional electrode improves the performance of the IDT sensors studied. In addition to the inter-electrode field, this ground electrode provides another electric field that is created between the electrode on the upper surface and the ground electrode. Fig. 15 shows the influence of the ground electrode on the electric field created in the piezoelectric plate for a case where $e < \lambda_{R\text{-}LAME}$. In this case, with this additional electric field, the amplitude of the displacement generated is much higher than without the ground electrode (Fig. 16).

Fig. 17 shows the maximum displacement amplitudes generated on the substrate by excitation of the IDT sensor. The excitation conditions are the same as previously (burst consisting of 10 sinusoids, $f_0 = 10$ MHz and $V_c = 20$ V). The blue curve is obtained for a sensor with a ground electrode and the green one for a sensor without a ground electrode. In both cases, the results are reported with the ratio between the piezoelectric plate thickness and the Rayleigh wave wavelength in the piezoelectric plate on the abscissa.

Again, it is possible to observe that maximum amplitudes are higher when the ratio $e/\lambda_{R\text{-}LAME}$ corresponds to $0.8 \cdot \lambda_{R\text{-}LAME} \leq e/\lambda_{R\text{-}LAME} \leq 1.2 \cdot \lambda_{R\text{-}LAME}$. In addition, the ground electrode only increases the displacement amplitude with a factor up to two, for small thicknesses (<100 µm). This is entirely logical since the electric field is inversely proportional to the distance between two dipoles. In the case of Pz29/aluminum, these small thicknesses correspond to ratios $e/\lambda_{R\_LAME} \leq 0.5$, which does not correspond to the best configuration. Thus, for the IDT studied, using a ground electrode does not really provide a positive contribution.

6. Experimental study

In order to validate the modeling results obtained, several IDT sensors were made from two PZT ceramics: Pz26 and Pz27 (Fig. 18).

The electrodes were made using two methods: a laser ablation-based method or an inkjet printing-based method, with dimensions

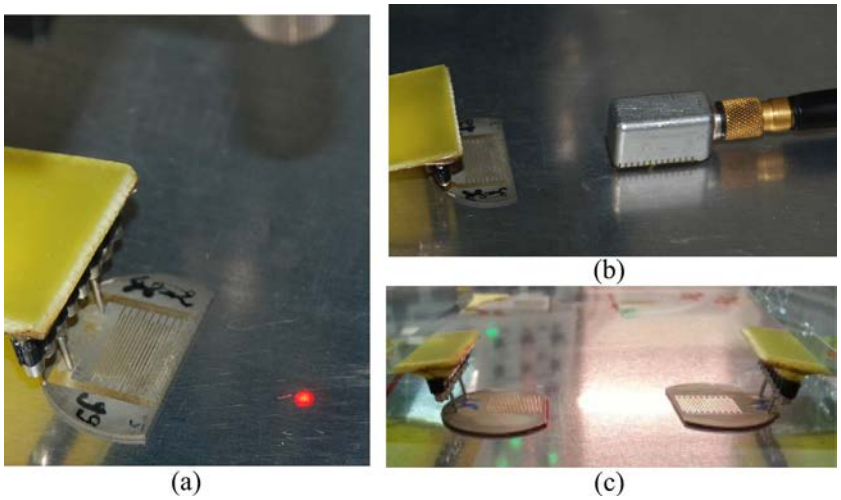

Fig. 18. Experimental set-up used to validate the design process (a) detection using interferometer, (b) detection using wedge sensor, (c) detection using another IDT sensor.

Table 2
Different parameters used to make IDT sensors.

Material	Frequency (MHz)	a = b (μm)	W (mm)	Number of electrodes
PZ26	4,3	169	8	20
PZ27	2,95	246	8	20

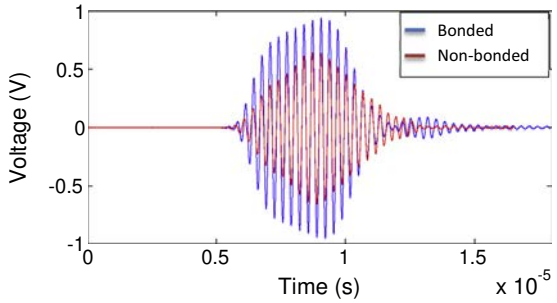

Fig. 19. Comparison of amplitude of SAW generated by an IDT sensor bonded and non-bonded on aluminum substrate.

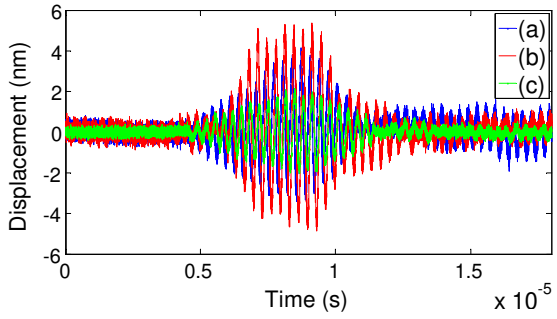

Fig. 20. Normal displacements of SAW, measured on aluminum substrate and generated by Pz27 IDT sensors (a) $e/\lambda_{R\text{-}LAME} = 0.33$ (b) $e/\lambda_{R\text{-}LAME} = 1$ (c) $e/\lambda_{R\text{-}LAME} = 1.7$.

to obtain IDT sensors with the desired resonant frequency [1]. The parameters of these electrodes are reported in Table 2.

A "burst" electrical excitation consisting of 10 sinusoids with a peak amplitude of 20 V was applied to the ten pairs of IDT sensor electrodes. For detection, three solutions were used. The first consisted in detecting the displacement using an interferometer, the second in using a wedge sensor and the third in using another IDT sensor. The absolute SAW displacement can be obtained directly with the first solution. Only results of the two first solutions are presented in this paper.

6.1. Characteristics of the contact between the IDT sensor and the substrate

Experimentally, the sensor can be either glued (permanently) to the structure, or put on the substrate via a couplant. These two configurations were tested on an aluminum substrate. Fig. 19 shows the results of the experiment for these two forms of binding, with Pz27/aluminum and a wedge sensor (at 10 mm of the IDT sensor) being used for detection. The signal recorded in both cases was comparable in shape, but contrary to the simulation, the amplitude was lower when the sensor was not bonded. This difference is probably due to the fact that in the simulation, the attenuation due to the couplant was not considered. However, since the amplitude is sufficient in both cases, we chose to perform the rest of the measurements using coupling in order to retain the possibility of using our sensors on other surfaces.

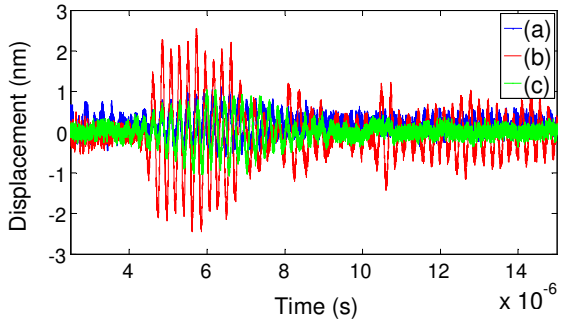

Fig. 21. Normal displacements of SAW, measured on aluminum substrate and generated by Pz26 IDT sensors (a) $e/\lambda_{R\text{-}LAME} = 0.43$ (b) $e/\lambda_{R\text{-}LAME} = 1$ (c) $e/\lambda_{R\text{-}LAME} = 2.15$.

6.2. Evaluation of the ideal thickness for the piezoelectric plate of an IDT sensor

In order to verify the best conditions for the ratio e/λ ($0.8 < e/\lambda < 1.2$), six IDT sensors with different ratios were tested. These IDT sensors had 20 electrodes. For the Pz27 ceramic, the $e/\lambda_{R\text{-}LAME}$ ratios were 0.33, 1 and 1.7, respectively. For the Pz26 ceramic, the $e/\lambda_{R\text{-}LAME}$ ratios were 0.43, 1 and 2.15, respectively. The displacements generated on the aluminum plate by SAW were recorded using a laser interferometer (at about 10 mm from the edge of the piezoelectric plate). Fig. 20 shows the results of the experiment for the three Pz27 IDT sensors and fig. 21 shows the results of the experiment for the three Pz26 IDT sensors. These results confirm that the displacements generated are greater when $e/\lambda_{R\text{-}LAME}$ is close to 1. These results are satisfactory and validate the numerical simulation results.

7. Conclusion

In this paper, the dimensional parameters of IDT sensors, for health monitoring of structures, were optimized using modeling and confirmed experimentally. After a quick reminder about the operating principle of IDT sensors, the modeling parameters were briefly presented. The parameters of IDT sensors for generating surface waves on non-piezoelectric substrates were studied by numerical simulation using the finite element method. Depending on the nature of the PZT ceramic, this study was used to determine the dimensions of the interdigital electrodes to be deposited (on the piezoelectric plate) to ensure optimal displacement amplitudes of the SAW in the substrate. The results obtained were used to make IDT sensors.

In conclusion, to generate SAW efficiently on substrate with PZT ceramic IDT sensor, it is necessary to satisfy two conditions. Firstly it is necessary to respect $a = \lambda_{R\text{-}sub}/4$. Secondly, the thickness of the piezoelectric plate must be comparable to the wavelength of SAW in the plate $0.8 \cdot \lambda_{R\text{-}LAME} \leq e/\lambda_{R\text{-}LAME} \leq 1.2 \cdot \lambda_{R\text{-}LAME}$.

Acknowledgments

We would like to thank Hauts-de-France region (CPER funds) and the European Union (Interreg program and FEDER funds) for supporting our research.

References

[1] R. Takpara, D. Fall, M. Duquennoy, M. Ouaftouh, C. Courtois, M. Rguiti, M. Gonon, N. Maurye, G. Martic, V. Lardot, L. Seronveaux, J. Halleux, C. Pélegris, M. Guessasma, Développement de capteurs interdigités pour le contrôle de structures, Leban. Sci. J. 16 (Special Issue) (2015) 69–80.

[2] J. Jin, S.T. Quek, Q. Wang, Design of interdigital transducers for cracks detection in plates, Ultrasonics 43 (2005) 481–493.
[3] Jeong K. Na, James L. Blackshire, Samuel Kuhr, Design, fabrication, and characterization of single-element interdigital transducers for NDT applications, Sensors Actuators A 148 (2008) 359–365.
[4] J. Deboucq, M. Duquennoy, M. Ouaftouh, F. Jenot, J. Carlier, M. Ourak, Development of interdigital transducer sensors for non-destructive characterization of thin films using high frequency Rayleigh waves, Rev. Sci. Instrum. 82 (2011) 1–7.
[5] F. Bellan Andrea Bulletti, Lorenzo Capineri, Leonardo Masotti, Goksen G. Yaralioglu, F. Levent Degertekin, B.T. Khuri-Yakub, Francesco Guasti, Edgardo Rosi, A new design and manufacturing process for embedded Lamb waves interdigital transducers based on piezopolymer film, Sensors Actuators A (2005) 123–124.
[6] Mohamed Badreddine Assouar, etude de dispositifs a ondes acoustiques de surface (saw) a structure multicouche nitrure d'aluminium/diamant: croissance de materiaux en couches minces et technologie de realisation, doctoral thesis, Université Henri Poincaré, Nancy I, 2001.
[7] Jeong K. Na, James L. Blackshire, Interaction of Rayleigh waves with a tightly closed fatigue crack, NDT&E Int. 43 (2010) 432–439.
[8] D. Royer, E. Dieulesaint, Onde élastique dans les solides, Tome 1, Propagation libre et guidée, Ed. Masson, 1996.
[9] D. Royer, E. Dieulesaint, Onde élastique dans les solides, Tome 2, Génération, interaction acousto-optique, applications, Ed. Masson, 1999.
[10] David P. Morgan, Surface-wave Devices for Signal Processing, Studies in Electrical and Electronic Engenieering, vol. 19, Elsevier, 1991.
[11] Ferroperm, High Quality Components and Materials for the Electronic Industry, Ferroperm Piezoceramics A/S.
[12] Sensortech, Piezoelectric Materials, Sensors Technology Limited©.
[13] Saint Gobain, Céramiques piézo-électriques, Saint Gobain©.